

Safer Roads Conference May 18-21, 2014, Cheltenham, UK

Towards Contactless Skid Resistance Measurement

Dr.-Ing. Andreas Ueckermann

Institute of Highway Engineering
RWTH Aachen University, Germany

General

Outline of the presentation

- Introduction
- Factors Influencing Skid Resistance
- Concept of Non-Contact Skid Resistance Measurement
- Rubber Friction
- Experimental Approach
- Results
- Conclusion

Introduction

Monitoring of Skid Resistance Today

- Skid resistance: important component of maintaining road networks
- Wide range of routine measurement devices existing
- Common feature: friction between tyre and (wet) road surface
- Example: SCRIM/ SKM



(Source: BASt)

Introduction

Attempts to predict skid resistance from texture measurements

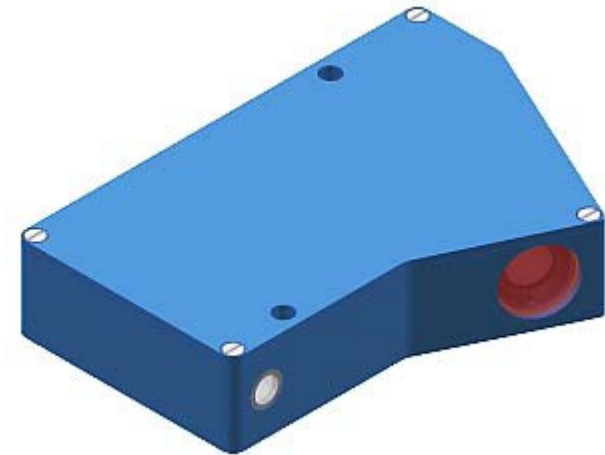
Amongst others:

- Schonfeld (1970) “Skid numbers from stereo-photographs”
- Ergün et al. (2005), “Prediction of road surface friction coefficient using only macro- and microtexture measurements”
- Dunford (2010), “Measuring skid resistance without contact”
- Basically three approaches:
 - Estimation from texture or texture related features/parameters gathered
 - Estimation via modeling (rubber contact, rubber friction, etc.)
 - Combined approach (e.g. Do et al. (2004), “Prediction of tire/wet grip road friction from road surface microtexture and tire rubber properties”)
- Reliable method to predict skid resistance from texture measurements still missing

Introduction

Idea

- Comparably **small** sensor
- Independent of **water** supply
- Independent of **tyre** (wear, temperature, etc.)
- Part of a **highly integrated** measurement system for monitoring the road net
- practically „unlimited“ **range**

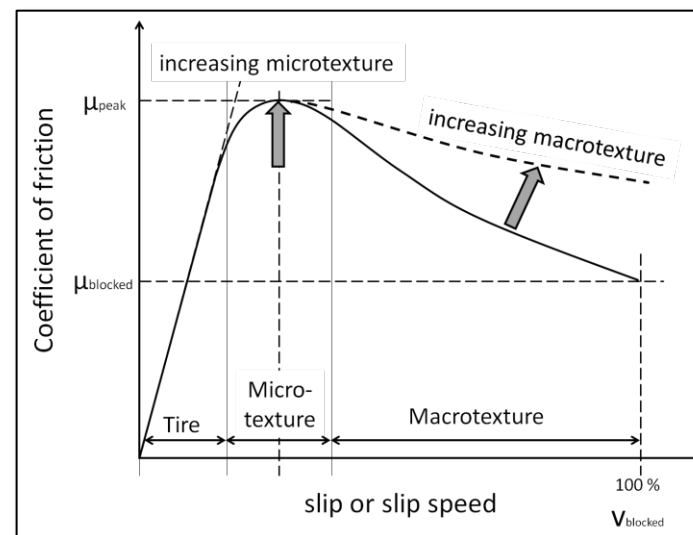


Factors influencing skid resistance

Influence of surface texture on skid resistance

- **tread stiffness** governs the increase of the μ -slip curve
- **microtexture** (wavelengths below 0.5 mm) governs the **peak** value
- **macrotexture** (wavelengths between 0.5 and 50 mm) governs its **decrease**

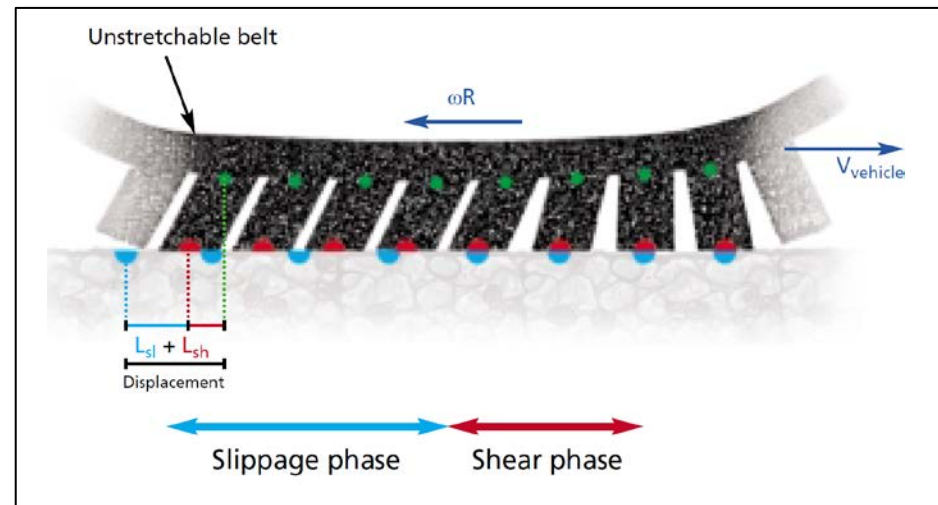
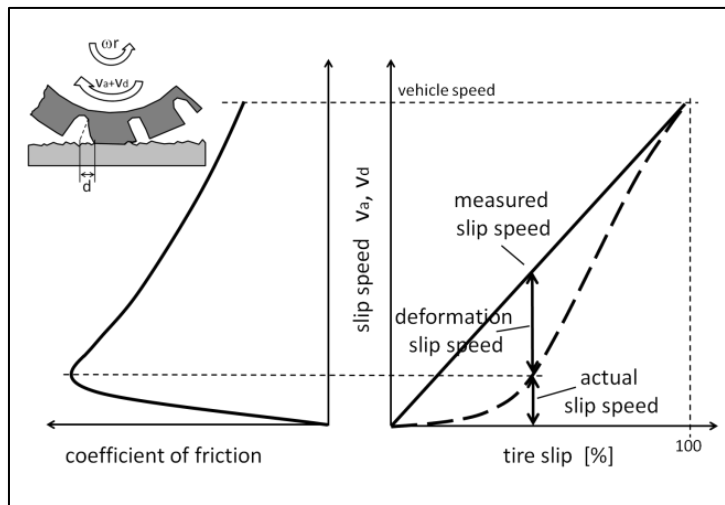
(wet) friction coefficient –
slip (or slip speed) curve



Factors influencing skid resistance

Real slip vs. deformation slip in the contact patch

- When skid resistance is measured under fixed slip conditions only part of the measured slip is due to pure sliding, the other part is caused by **deformation**
- Different slip conditions are encountered within the contact patch

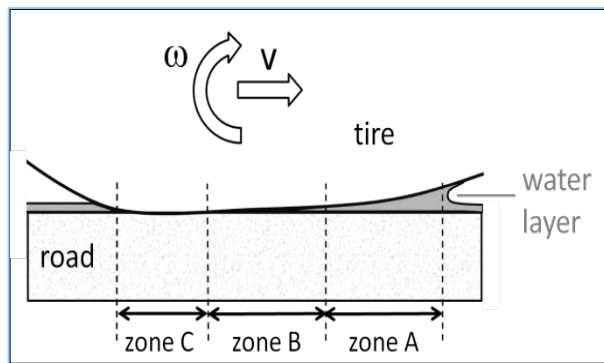


Source: Michelin

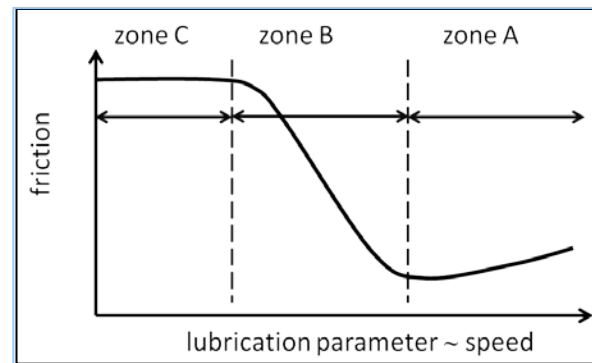
Factors influencing skid resistance

Influence of water on contact conditions and generable traction

- A) “sinkage” or “squeeze-film” zone (water separates the two surfaces)
- B) “draping” or “transition” zone (tread elements commence to “drape” over the major asperities)
- C) “contact” or “traction” zone (boundary lubrication regime, dry contact estd.)



Three-zone-model acc. to Moore



Stribeck Curve – describing lubrication regimes

Factors influencing skid resistance

Factors influencing traction/ skid resistance

- **Vehicle** (axle load distribution, split-up of brake power, center of gravity, wheel alignment, etc.)
- **Tyre** (dimension, construction, material, tread depth, tread design, inflation pressure, tire temperature, etc.)
- **Driving mode** (braking, acceleration, cornering, speed, etc.)
- **Surface and ambient conditions** (dry, wet, water depth, contamination, snow, ice, ambient temperature, etc.)
- **Pavement** (material, microtexture, macrotexture, drainage capacity, etc.)

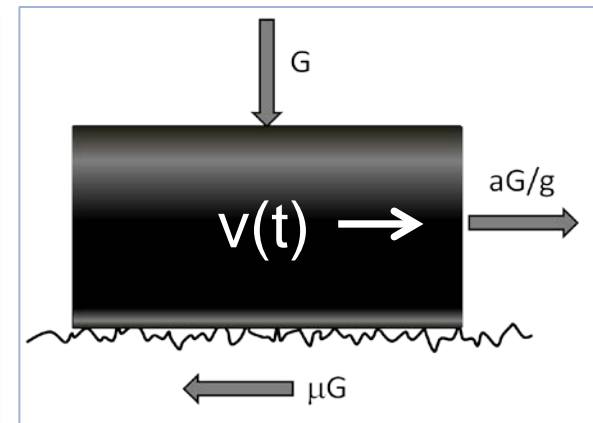
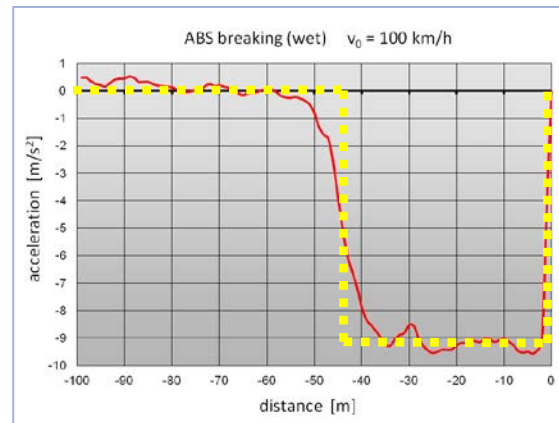
Concept of non-contact skid resistance measurement

Analogy

Despite of numerous influencing factors:

- ABS wet braking resembles deceleration of a single mass
- There is a close relation between deceleration and coefficient of friction
- Analogy between braking and rubber block sliding on a rough rigid substrate suggests to calculate skid resistance by means of a **rubber friction model**

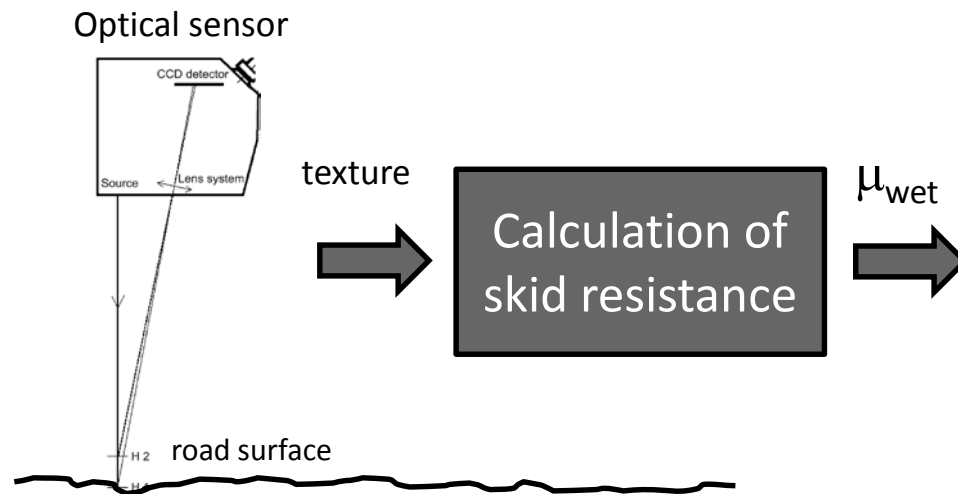
deceleration as
a function of
braking distance
(ABS-braking
on wet road)



Concept of non-contact skid resistance measurement

Two-step “measuring” concept

- **Measurement** of the pavement texture by means of an optical measuring system
- **Calculation** of skid resistance by means of a rubber friction model based on texture



Rubber friction

Components of rubber friction

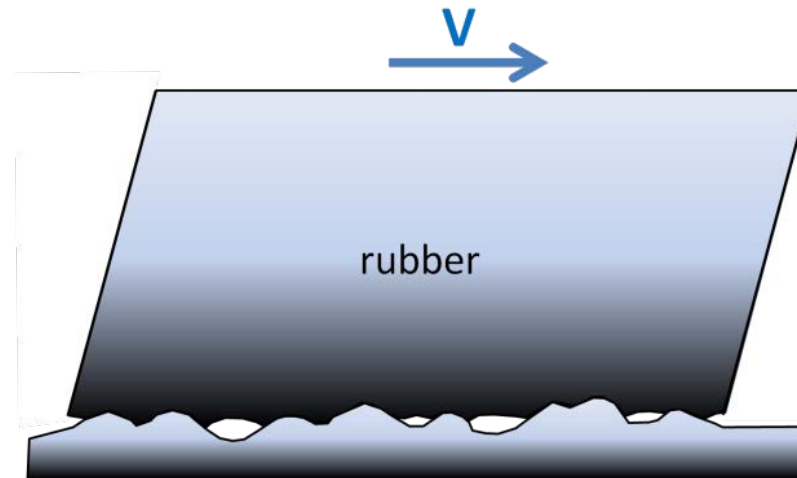
- **Hysteresis** component - results from internal friction of the rubber. During sliding over a rough surface the asperities exert oscillating forces on the rubber resulting in energy dissipation due to internal damping of the rubber
- **Adhesion** component - results from attractive binding forces between the rubber surface and the substrate. Important only for clean, smooth surfaces and small sliding velocities
- **Cohesion** component - represents the energy required to produce new surfaces. Associated with grooving of the rubber and abrasive wear
- **Viscous** component - arises from shearing of a viscous layer between tyre and road surface. Can occur only on wet roads.

Rubber friction

Main factors determining rubber (hysteresis) friction

Consider a tread block sliding over a rigid substrate: The friction depends on

- **Texture in the contact patch**
- **Material behaviour of rubber**
 - viscoelastic properties
 - thermal properties
- **“Loading” conditions**
 - nominal contact pressure
 - ambient temperature
 - sliding velocity

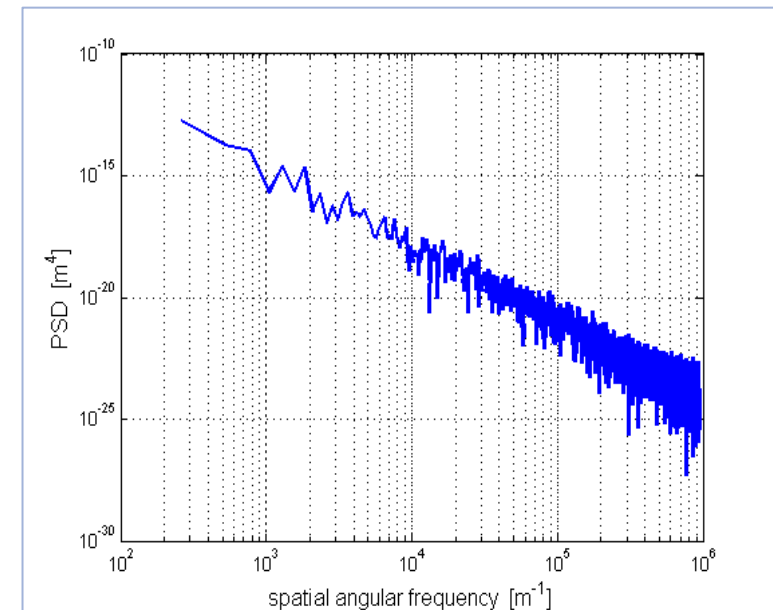


Rubber friction

Description of the surface texture

- Contact concentrates on the top of the stones
- Stones are broken material exhibiting
 - “fractal” appearance
 - roughness over several length scales
- Many road surfaces nearly **self-affine**
 - “look the same” when studied under magnification different in vertical and lateral magnification

Power Spectral Density



Rubber friction

Description of the surface texture

- The power spectral density of self-affine surfaces follows a **power law**

$$C(q) \sim q^{-2(H+1)}$$

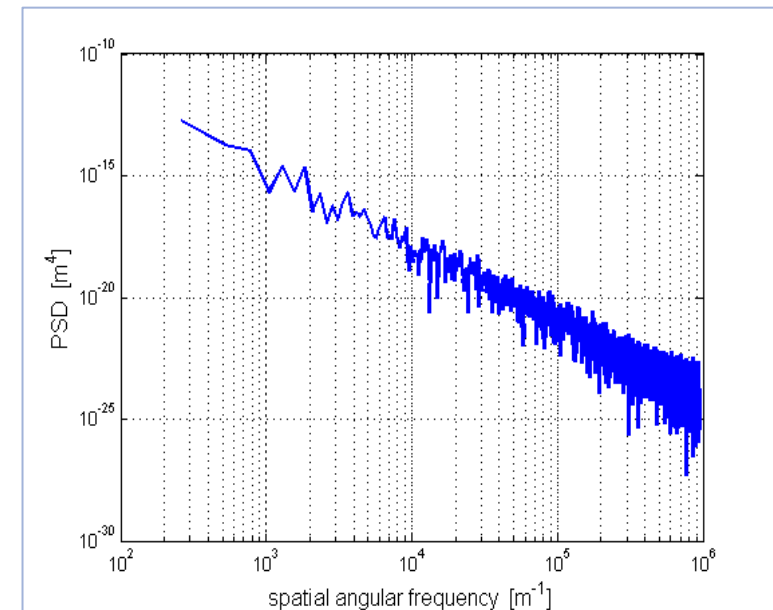
where q := spatial angular frequency
 $q = 2\pi/\lambda$ with λ := wavelength
 H := Hurst exponent

- The Hurst exponent is related to the fractal dimension D_f via

$$H = 3 - D_f$$

- The power law corresponds to a linear shape when displayed in a log-log scale

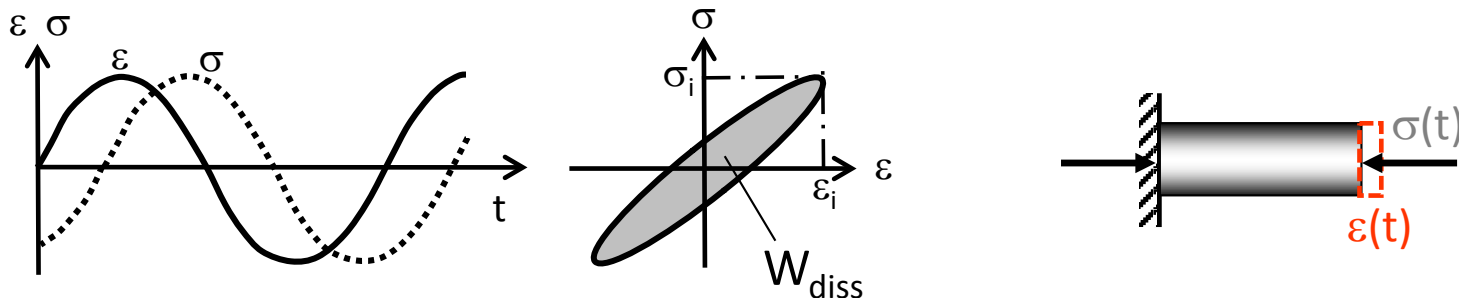
Power Spectral Density



Rubber friction

Description of the viscoelastic behaviour

- When a **sinusoidal loading** is applied to a piece of rubber a phase shift between strain and stress can be observed
- In the strain-stress diagram a so called **hysteresis curve** can be observed
- The area enveloped by the hysteresis curve is a measure for **the energy dissipated** in the rubber during loading

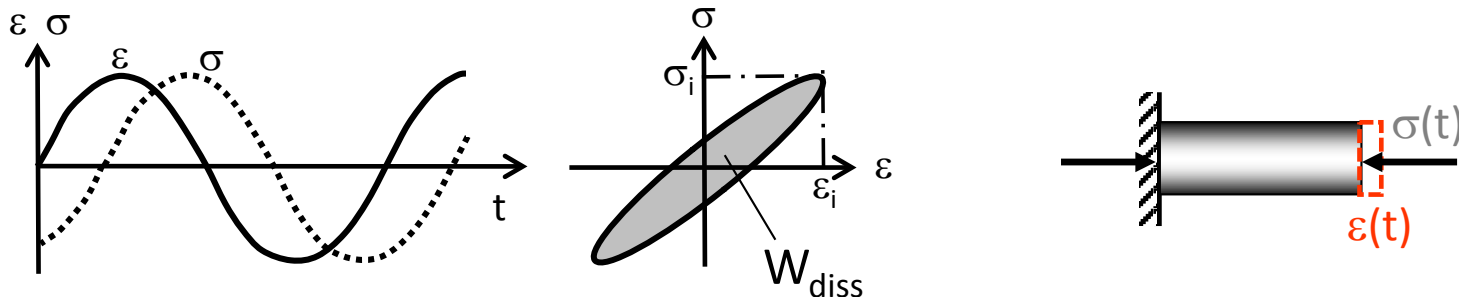


Rubber friction

Description of the viscoelastic behaviour

- The phase shift and ratio of stress and strain is a function of the loading frequency
- This frequency-dependent viscoelastic behavior of rubber can be described by a complex elastic modulus

$$\sigma(j\omega) = E(j\omega) \cdot \epsilon(j\omega)$$



Rubber friction

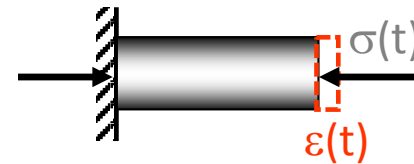
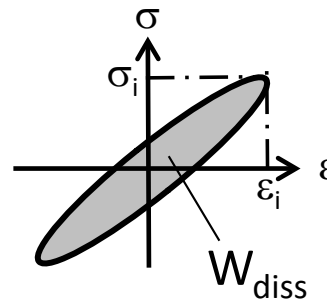
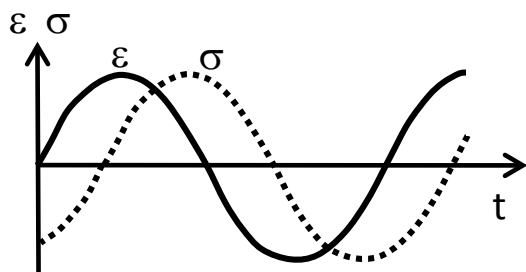
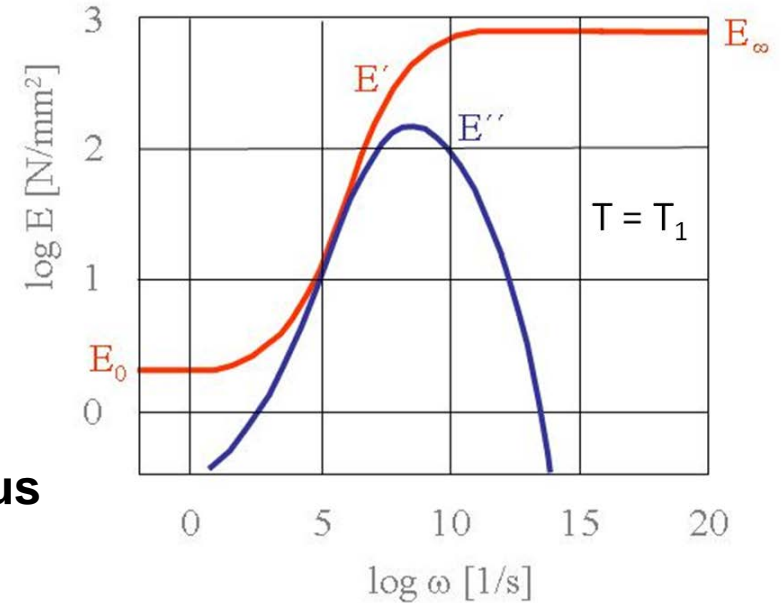
Description of the viscoelastic behaviour

- The complex modulus can be written

$$E(j\omega) = E'(\omega) + jE''(\omega)$$

the real part $E'(\omega)$ is called **storage modulus**

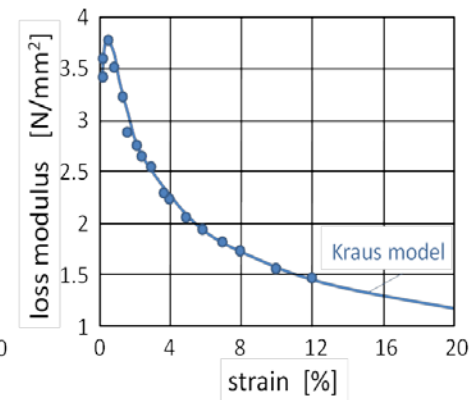
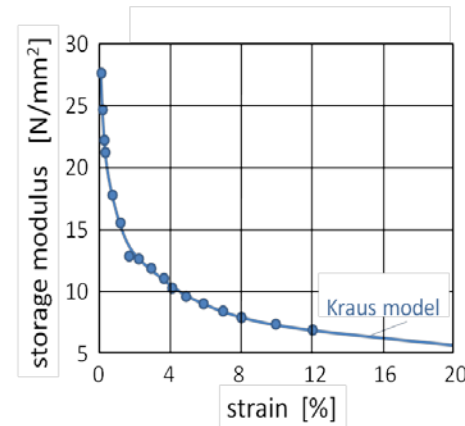
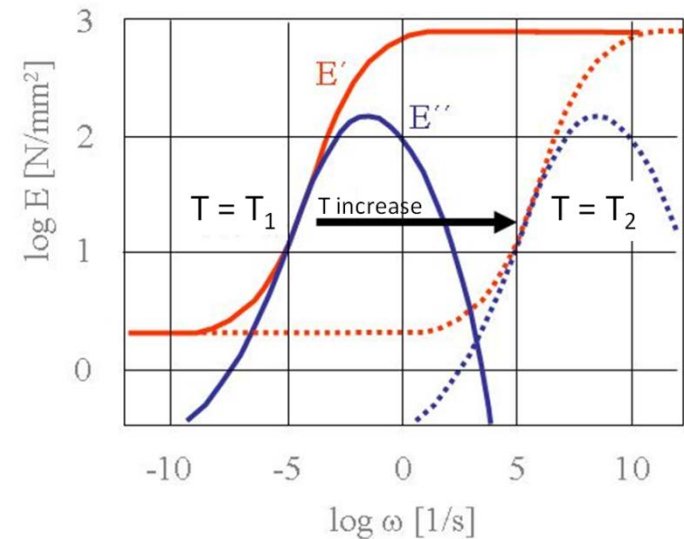
the imaginary part $E''(\omega)$ is called **loss modulus**



Rubber friction

Description of the viscoelastic behaviour

- The complex modulus of elasticity of rubber is dependent on
 - **frequency**
 - **temperature**
 - **strain**
- **temperature** influence: shift along the frequency axis (temperature-frequency equivalence, Williams-Landel-Ferry (WLF) equation)
- **strain** influence e.g. by “Kraus” model (strain increase – decreasing modulus)



Rubber friction

Persson's model for hysteresis friction

- For the calculation of skid resistance from texture we used the **Persson model**
- The **coefficient of friction** according to Persson is proportional to an integral containing three major factors

$$\mu \sim \int_{q_L}^{q_H} C(q) P(q) E''(q) q^3 dq$$

$C(q)$ is the two-dimensional power spectral density

$P(q)$ is the frequency-dependent contact function and

$E''(q)$ is the loss modulus of the rubber

q is the spatial angular frequency $q = 2\pi/\lambda$ where λ is the wavelength

q_L, q_H is the lower and upper cutoff frequency representing a wavelength range extending from a micrometer scale to a millimeter scale

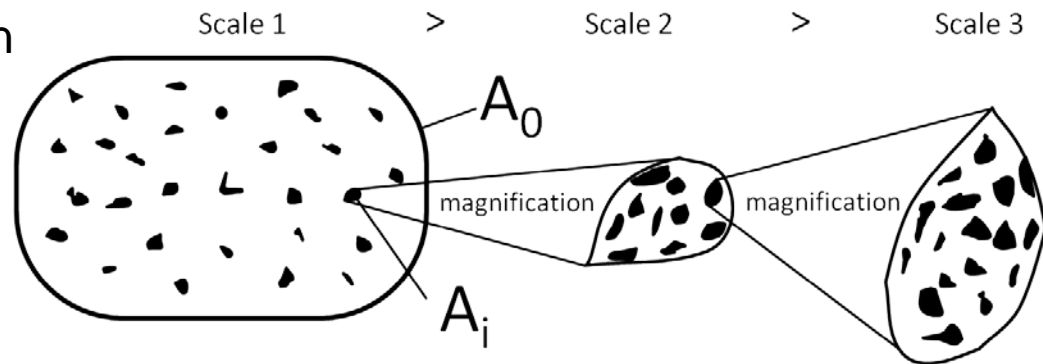
Rubber friction

Persson's model for hysteresis friction

- The contact function $P(q)$ is defined as the ratio of real and nominal (macroscopic) area of contact, A_0 , where the surfaces are **considered smooth on spatial frequencies higher than q**

$$P(q) = \frac{A(q)}{A_0}$$

- According to this definition the real area of contact becomes smaller the closer we look at a contact spot



Rubber friction

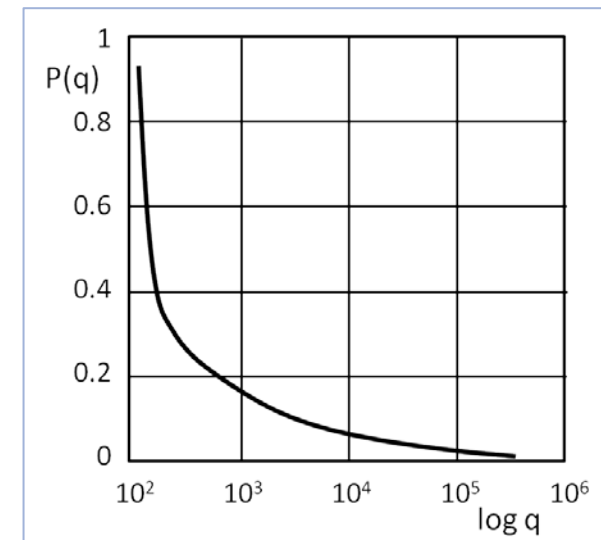
Persson's model for hysteresis friction

- The contact is a function of the **magnification** we use to study it – or in other words – the scale, which in turn can be expressed by the spatial angular frequency q

$$P = P(q)$$

- Physically, it is determined by
 - texture** in the contact patch
 - material behaviour** of rubber
 - viscoelastic properties
 - thermal properties

Contact function $P(q)$



Rubber friction

Persson's model for hysteresis friction

- Physically, it is determined by
 1. “loading” conditions
 - nominal contact pressure
 - ambient temperature
 - sliding velocity

- It can be expressed by

$$P(q) = \frac{2}{\pi} \int_0^\infty dx \frac{\sin x}{x} \exp(-x^2 G(q))$$

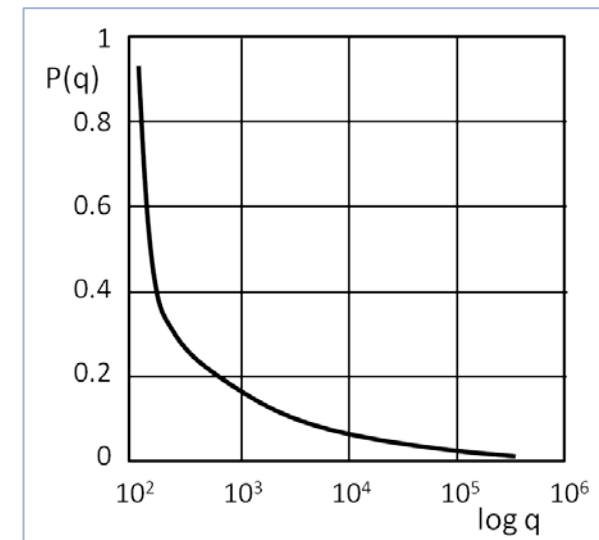
where

$$G(q) = \frac{1}{8} \int_{q_L}^q dq q^3 C(q) \int_0^{2\pi} d\phi \left| \frac{E(qv \cos \phi)}{(1 - v^2)\sigma_0} \right|^2$$

$P(q)$ depends on

- v, σ_0
- v and $|E(qv)| = |E(\omega)|$
- $C(q)$

Contact function $P(q)$



Rubber friction

Persson's model for hysteresis friction

- As mentioned above the texture power spectral density $C(q)$ contains a **broad band** of amplitudes and frequencies
- The part of it which comes into contact and determines the hysteresis losses, is

$$C_{eff}(q) = P(q) \cdot C(q)$$

- This part of the texture penetrates the rubber and causes hysteresis losses in a broad band of excitation frequencies covering several length scales from (typically) several micrometers to several millimeters

Rubber friction

Persson's model for hysteresis friction

- The hysteresis losses in each frequency band need to be summarized to give the total energy loss during sliding
- The energy dissipated related to the energy used to establish the contact results in the expression for the coefficient of friction

$$\mu_k = \frac{1}{2} \int_{q_L}^{q_1} dq q^3 C(q) P(q) \int_0^{2\pi} d\phi \cos \phi \operatorname{Im} \frac{E(qv \cos \phi)}{(1 - \nu^2) \sigma_0}$$

σ_0 is the nominal (macroscopic) contact pressure

ν is Poisson's ratio which can be set to 0.5 for rubber

ϕ is the angle between sliding direction and particular wave vector q

qv is the angular frequency $\omega = 2\pi f$ caused by the sliding velocity v

Rubber friction

Application of the rubber friction model

- Two different skid resistance devices have been represented by the rubber friction model:
- **Wehner-Schulze**-device
a laboratory device simulating a **blocked-wheel** braking
- **ViaFriction**[®] by ViaTech AS, Norway
a road and airfield measuring device measuring under slip conditions **similar to ABS braking**
- road surfaces relatively rough - wet conditions - comparatively high sliding velocities ' **hysteresis** dominating friction mechanism; adhesion neglected

Rubber friction

Application of the rubber friction model

The following **assumptions** have been made for the rubber friction model:

- the frictional process generated by the skid resistance measuring devices can be described by a **steady-state** process characterized by a average sliding velocity
- the steady-state process is characterized by an “**operating**” **temperature** of the rubber in the vicinity of the contact zone which determines its viscoelastic properties
- the **water** acts as a **coolant** and ensures moderate tire temperatures compared to dry friction

Rubber friction

Application of the rubber friction model

Assumptions cont'd

- the **contact conditions** correspond to the **boundary lubrication** regime where in parts dry contact can be established
- **hysteresis** is the dominating friction mechanism
- **adhesion** can be neglected due to sliding velocities, pavement roughness and water film
- **viscous effects** are insignificant compared to hysteretic effects
- the **water** acts as a low-pass **filter** limiting the wavelengths the tire can follow in the high frequency range (sealing and expulsion constraints)

Rubber friction

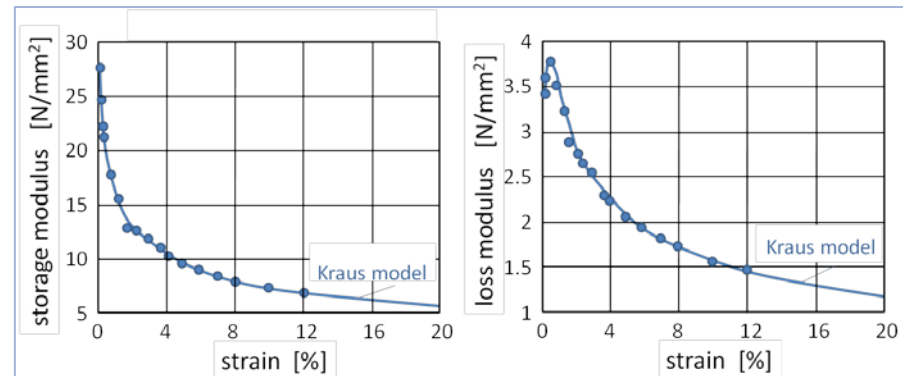
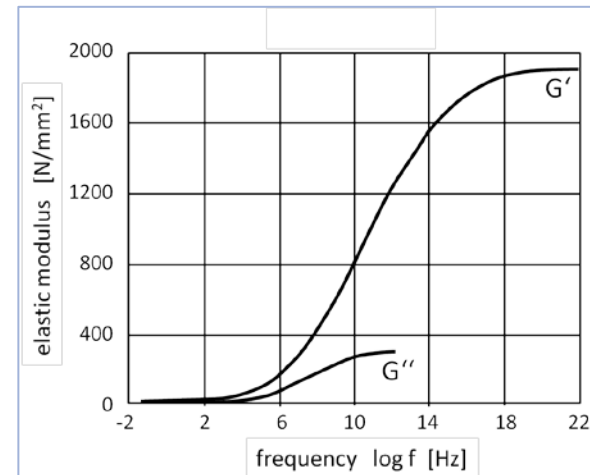
Application of the rubber friction model

- no information about the rubber properties of the measuring devices
- we used measured master curves of an actual tread rubber which were provided to us by a major tire manufacturer
- temperature dependence is allowed for by the Williams-Landel-Ferry equation (knowing that it should be restricted to unfilled rubbers)
- However, as a first attempt to explore the potential of the theory of rubber friction for contactless skid resistance prediction we used this approach ...
- assuming that for an appropriate frequency band - temperature constellation a behavior similar to that of the respective measuring rubbers could be found

Rubber friction

Application of the rubber friction model

- Measured master curves
(Temp: 20 °C; strain: 0.2 %)
- Measured dependency of
modulus on strain
(Temp: 20 °C; Freq: 10 Hz)



Rubber friction

Application of the rubber friction model

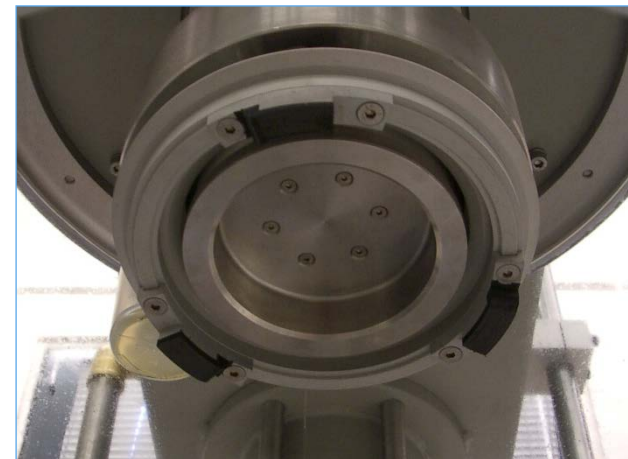
- The best agreement between calculated and measured friction coefficients was obtained with the following parameter settings

Parameter Settings	
Considered wavelength range	20 μm to 25 mm
Contact pressure	0.2 N/mm^2
Poisson's ratio	0.5
Average strain	8 %
Sliding velocity	60 km/h (Wehner/Schulze)
	12 km/h (ViaFriction®)
Rubber temperature in the contact zone	57 °C (Wehner/Schulze)
	47 °C (ViaFriction®)
Wavelengths treated decisive for the friction	60 μm to 1 mm (W/S)
	20 μm to 1 mm (ViaFriction®)

Experimental approach

Wehner-Schulze device

- consists of a rotating head equipped with 3 rubber pads which are arranged equiangular around a metal rim
- the head is lifted from the pavement sample and accelerated to a rim speed of 100 km/h
- the water supply is activated and the rotating head released. It drops onto the sample and is decelerated due to friction between rubber and specimen
- The friction coefficient is recorded



Experimental approach

ViaFriction device

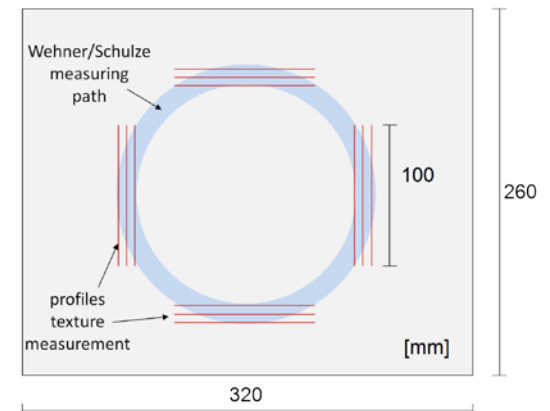
- consists of a measuring trailer and a towing vehicle containing the water tank
- The measuring unit features a wheel which can be run under controlled slip
- Different slip modes (variable, constant) can be chosen
- We used 20 % slip and a measuring speed of 60 km/h.



Experimental approach

Texture measurements

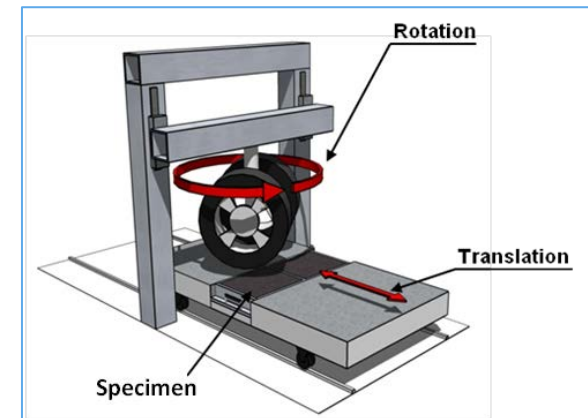
- were conducted in laboratory with a chromatic white-light sensor
- Resolution
 - lateral: $3.3 \mu\text{m}$
 - vertical: 20 nm
- 12 profiles were measured in the path of the Wehner-Schulze device
- Based on these 12 profiles the power spectral density characterizing the sample texture was calculated



Experimental approach

Polishing treatment to enlarge the number of samples

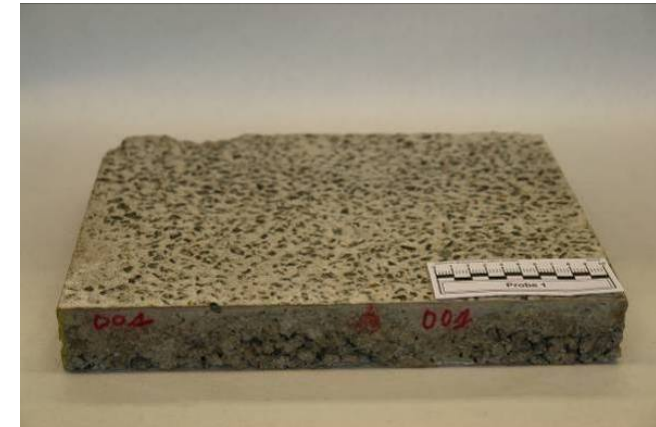
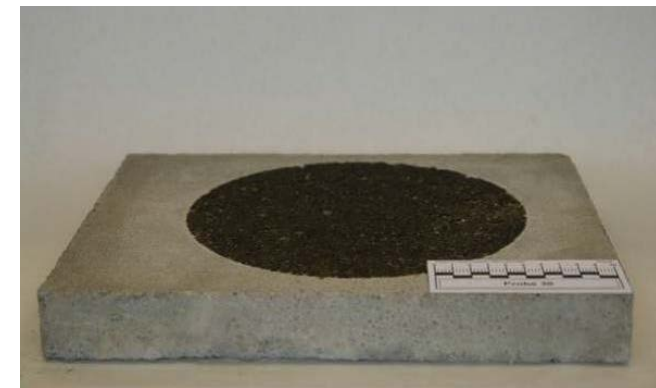
- was conducted by means of the Aachen Rafeling Tester (ARTe)
- features a pair of passenger car wheels which are moved across the specimen surface in a combined rotational and translational motion
- tires of dimension 165/75 R14 are operated with a tire pressure of 2 bar. The load is 1500 N.
- mixture of polishing agents and water was applied to accelerate wear.



Results

Comparison between measured and calculated skid resistance (Wehner-Schulze)

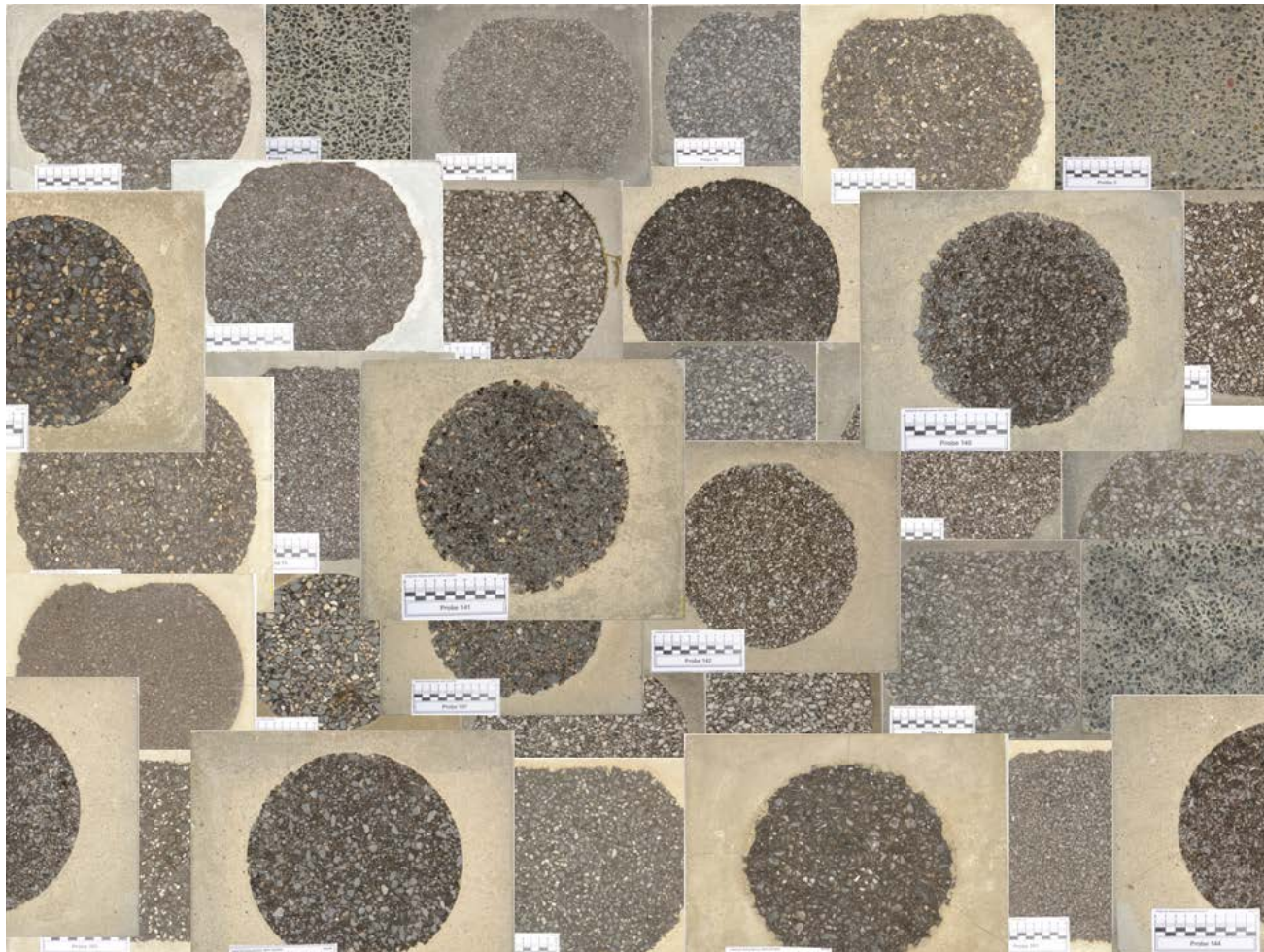
- For comparison with the Wehner/Schulze device 33 different surfaces have been tested.
- 13 of them were **washed concrete slabs** made in the laboratory exhibiting different maximum aggregate sizes (8 and 11 mm) and different polishing treatments to enlarge the sample number
- 20 of them were **asphalt cores** obtained from actual road surfaces and parking lots comprising maximum aggregate sizes between 8 and 11 mm
- 2 samples per surface were available on average (70 samples in total)



Results

Comparison between measured and calculated skid resistance (Wehner-Schulze)

Visual
impression
of the
variety of
surfaces



Results

Comparison between measured and calculated skid resistance (Wehner-Schulze)

Overview

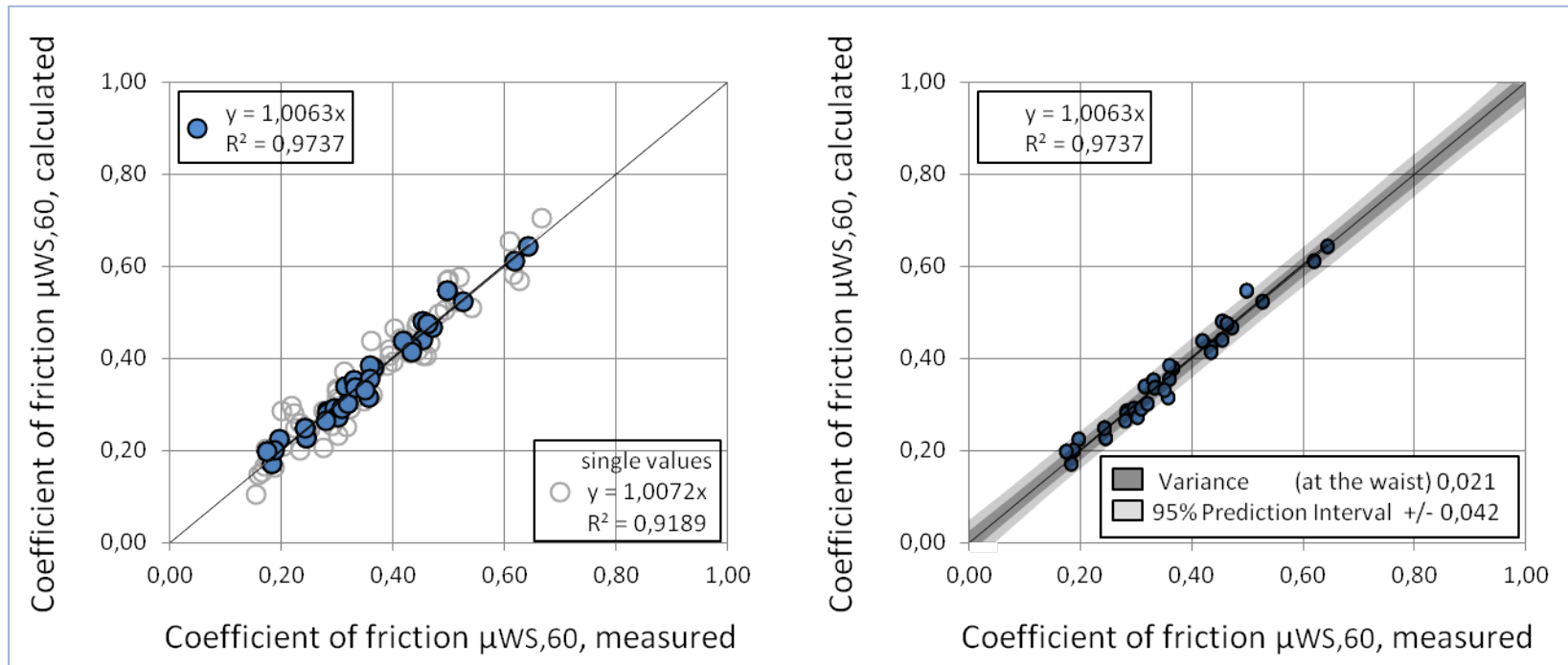
- 19 surfaces: Asphalt Concrete pavements
- 1 surface: Stone Mastic Asphalt
- 13 surfaces: Washed Concrete, sandblasted and subsequently polished in different stages
- the **polishing** was conducted with the Aachen Rafeling Tester (ARTe)

No.	$\mu_{WS,60}$ measured	$\mu_{WS,60}$ Theory	sample size	surface example	origin/details
1	0,43	0,42	2		laboratory sample, initial state
2	0,62	0,61	2		laboratory sample, sandblasted
3	0,42	0,44	2		laboratory sample, polishing stage 1
4	0,43	0,41	2		laboratory sample, polishing stage 2
5	0,45	0,44	2		laboratory sample, initial state
6	0,64	0,64	2		laboratory sample, sandblasted
7	0,47	0,47	2		laboratory sample, polishing stage 1
8	0,45	0,48	2		laboratory sample, polishing stage 2
9	0,36	0,31	2		laboratory sample, initial state
10	0,53	0,52	2		laboratory sample, sandblasted
11	0,32	0,34	2		laboratory sample, polishing stage 1
12	0,37	0,38	2		laboratory sample, polishing stage 2
13	0,24	0,25	4		Aachen, Goethestraße 13
14	0,20	0,22	2		Aachen, Boxgraben 22, initial state
15	0,18	0,17	2		Aachen, Boxgraben 22, polishing stage 1
16	0,19	0,20	2		Aachen, Boxgraben 22, polishing stage 2
17	0,17	0,20	4		Aachen, Lütticher Straße 21
18	0,30	0,28	1		Aachen, Wallstraße 57
19	0,30	0,29	2		Aachen, Lütticher Straße 56, right lane
20	0,24	0,23	4		Aachen, Lütticher Straße 56, left lane
21	0,28	0,28	1		Aachen, Boxgraben 32
22	0,28	0,28	1		Aachen, Lütticher Straße 21, bicycle lane
23	0,33	0,35	3		Aachen, Rüd. Ring, road surface
24	0,50	0,55	3		Aachen, Rüd. Ring, adjacent areas
25	0,36	0,38	1		Aachen, Madrider Ring
26	0,30	0,27	2		Eschweiler (36+37), left and right lane
27	0,28	0,26	1		Aachen, parking lot, coarse aggregate
28	0,31	0,29	2		Aachen, parking lot, fine aggregate
29	0,32	0,30	2		Aachen, parking lot
30	0,36	0,35	2		Aachen, parking lot
31	0,33	0,34	2		Aachen, parking lot
32	0,35	0,33	1		Aachen, Schleidener Straße
33	0,46	0,47	4		laboratory sample, Exposed aggregate concrete

Results

Comparison between measured and calculated skid resistance (Wehner-Schulze)

- Close agreement between measured and calculated coefficients of friction ($\mu_{WS,60}$ is the Wehner-Schulze coefficient of friction at a velocity of 60 km/h)

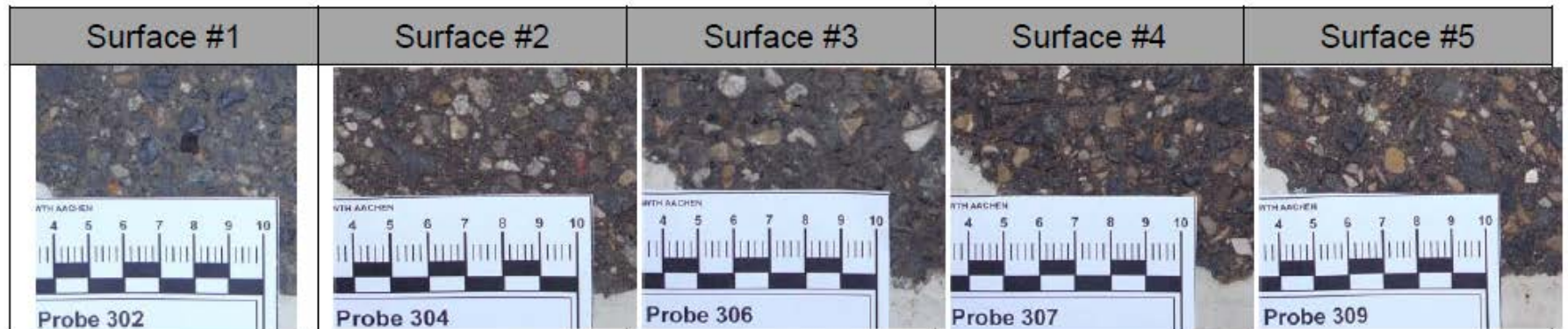


Results

Comparison between measured and calculated skid resistance (ViaFriction)

- For comparison with the ViaFriction device unfortunately only 5 different surfaces were available
- Further, the friction coefficients were relatively close together
- 2 core samples per surface

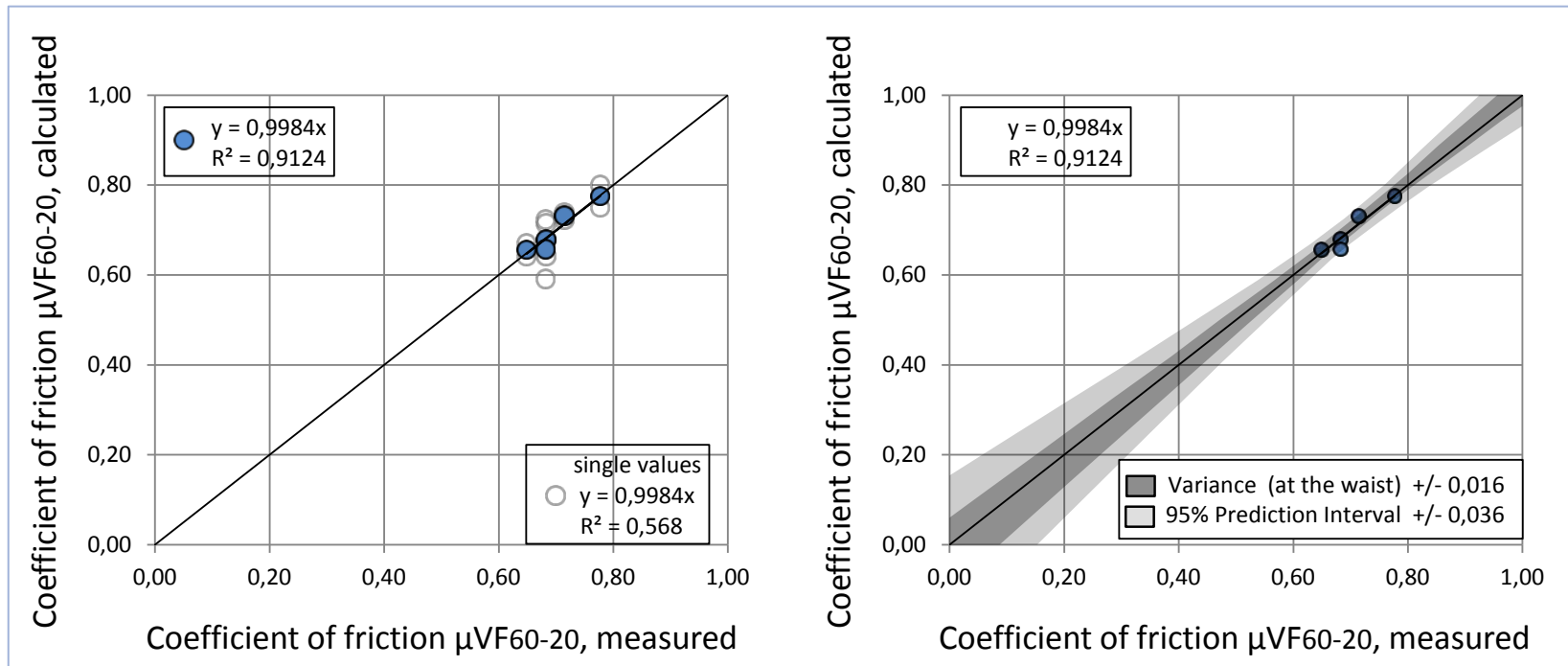
No.	Internal No.	$\mu_{VF60-20}$ measured	$\mu_{VF60-20}$ calculated	number of samples	pave-ment	details/origin
1	301/302	0,71	0,73	2	SMA 0/8	B56 dir. Puffendorf; Station 1+200 left, section 15.2
2	303/304	0,65	0,66	2	SMA 0/8	B56 dir. Aldenhoven; Station 1+200 right, section 15.2
3	305/306	0,78	0,78	2	SMA 0/11	B55 dir. Elsdorf; Station 2+400 right, section 5
4	307/308	0,68	0,68	2	AC 0/11	L366 dir. Hompesch; Station 0+600 right, section 1
5	309/310	0,68	0,66	2	AC 0/11	L366 dir. A44; Station 0+600 left, section 1



Results

Comparison between measured and calculated skid resistance (ViaFriction)

- Close agreement between measured and calculated coefficients of friction ($\mu_{VF,60}$ is the ViaFriction coefficient of friction at a velocity of 60 km/h)



Conclusion

Conclusion (I)

- Close agreement between measured and calculated coefficients of friction could be attained
- The parameter settings for both, Wehner-Schulze and ViaFriction device seem to be reasonable:
- 60 °C is a typical tire temperature during driving on a dry road; on a wet road due to liquid cooling the temperature is typically around 30° C. So, **rubber temperatures** of 57 °C (Wehner-Schulze) and 47 °C (ViaFriction®) can be expected as an average in the vicinity of contact spots under wet sliding conditions.

Conclusion

Conclusion (II)

- the friction process in the W-S machine is associated with higher **temperatures** than the friction process in the ViaFriction® device because of the higher sliding velocities involved (100 – 0 km/h compared to 12 km/h).
- for the ViaFriction® device the decisive **wavelength range** extends to smaller wavelengths than for the W/S machine (20 micrometer compared to 60 micrometer). Because of the lower sliding velocity the ViaFriction® rubber is able to follow smaller wavelengths. The W/S machine on the contrary is associated with higher velocities (up to 100 km/h), smaller expulsion periods and possibly more water volume involved in the friction process which has to be expelled.

Conclusion

Note

- These conclusions, however, are based on the assumption that both devices are equipped with the same rubber which, in fact, is not the case. So, in reality, the different friction levels are influenced by the (different) rubber properties as well.
- For lack of information about the regarding rubber properties we used measured master curves of an actual tread rubber which were provided to us by a tyre manufacturer.
- **first attempt** to explore the potential of the theory of rubber friction for contactless skid resistance prediction, assuming that for an appropriate frequency band - temperature constellation a behavior similar to that of the respective measuring rubbers could be found. The results seem to confirm this assumption. Nevertheless, further work should be founded on a better empirical basis.

Thank you very much.